

Nonlinear dynamics of vortexlike domain walls in magnetic films with in-plane anisotropy

B. N. Filippov, L. G. Korzunin, and F. A. Kassan-Ogly

Institute of Metal Physics, Ural Division, Russian Academy of Sciences, ul. S. Kovalevskoi 18, Ekaterinburg, 620219, Russia

(Received 8 September 2000; published 21 August 2001)

The nonlinear nonstationary dynamics of domain walls with variable two-dimensional internal structure (topological solitons with internal degrees of freedom) under the action of an external magnetic field was investigated in magnetic films having an in-plane anisotropy and a small damping coefficient α . The iteration calculation procedure of the temporal evolution of the magnetization distribution is based on the predictor-corrector method for direct numerical solution to the Landau-Lifshitz equations. The variable time step procedure was employed. It is shown that along with the periodic change of the internal structure of a wall occurring with a certain period T there also appear the subperiodic vibrations of some parts of the walls relative to the other parts which results in the high-frequency oscillations ($\approx 10^{11}$ Hz) of the velocity of a domain wall in the fields above some critical field H_c at a small damping. The dependence of the period of dynamic rearrangement of the internal structure of the walls on the external magnetic field and damping was studied. The singular dependence of T on H is established to be different from the $(H^2/H_c^2 - 1)^{-1/2}$ law which is typical of one-dimensional models of a wall. The dependence of H_c on α is evaluated and appears to differ substantially from that of the one-dimensional models.

DOI: 10.1103/PhysRevB.64.104412

PACS number(s): 75.60.Ch, 05.45.-a, 87.17.Aa

I. INTRODUCTION

The internal structure of domain walls in magnetic uniaxial films is known to be not one dimensional in the general case.¹ This imposes an essential influence on their dynamic behavior. Two particular cases should be distinguished: the films with perpendicular magnetic anisotropy and the films in which an easy axis lies in their plane (an in-plane anisotropy). Previously most of the papers were devoted to the films with perpendicular anisotropy. This is related not only to their practical applications but also to the contribution of magnetostatic fields to the total energy, which is most difficult to compute and can be taken into account approximately due to a great quality factor $Q = K/2\pi M_s^2$ (K is the uniaxial anisotropy constant, M_s is the saturation magnetization). The magnetostatic contribution proves to be the main one and should be taken into account rigorously. Rigorous account of basic interactions, including the dipole-dipole one, reveals the asymmetric structure of domain walls in the framework of a two-dimensional model of magnetization distribution.^{2,3} Such domain walls are realized, for instance, in Permalloy films 0.04–0.2 μm thick. The existence of these walls is confirmed experimentally.^{4–6} The switching on of the external magnetic field along an easy axis of magnetization leads not only to a displacement of the domain wall but also of a vortex in it. Thus, from the viewpoint of nonlinear physics there is a very interesting object, namely, a topological soliton with internal degrees of freedom. An advance in the studies of such objects was connected with the work by Yuan and Bertram,⁷ in which the substantial periodic transformations in the internal structure of a domain wall were shown to occur in sufficiently high fields. The effect of various film parameters on the character of these transformations was elucidated in our previous papers.^{8,9} It revealed the important properties of the critical field H_c , above which the motion of a domain wall is accompanied by a periodic rearrangement of its internal struc-

ture. In particular, it was established that the one-dimensional models of domain walls could not describe the properties of H_c .

However, in all the works cited only films with sufficiently high damping $\alpha \geq 0.02$ (α is the Gilbert damping parameter) were considered. This restriction is related to the fact that at much lower α values the critical field becomes small, and a period T of rearrangement of the internal structure becomes very large and inevitably needs great computation time. This circumstance imposes severe restrictions on the numerical experiments. At the same time, it is just a great period T that is favorable for experimental studies, since no problems concerning the temporal resolution appear in this case. Moreover, a wall motion is impossible in the absence of damping due to the gyrotropic properties of elementary magnetic moments. Thereby a question appears of how the nonlinear dynamic behavior of a wall would change as the damping becomes small. In the present paper the nonlinear and, in the general case, nonstationary dynamics of domain walls with a two-dimensional distribution of magnetization is considered at a small damping. In order to solve this problem we advanced our previous computation programs by introducing a variable time step.

II. STATEMENT OF THE PROBLEM AND BASIC EQUATIONS

Let us consider a uniaxial magnetic film of thickness b with a surface parallel to the x - y plane and an easy axis directed along the z axis (see Fig. 1). Let the magnetic state of this film correspond to two domains with uniform saturation magnetization $\pm M_s$, oriented along $+z$ ($-z$) at $x > a/2$ ($x < -a/2$). We assume that a domain wall is entirely located in a region V with a rectangular cross section D in the x - y plane and a length a along the x axis. Assume also that $\mathbf{M} = \mathbf{M}(x, y)$ in this region V , which corresponds to a two-dimensional model of \mathbf{M} distribution. In one-dimensional

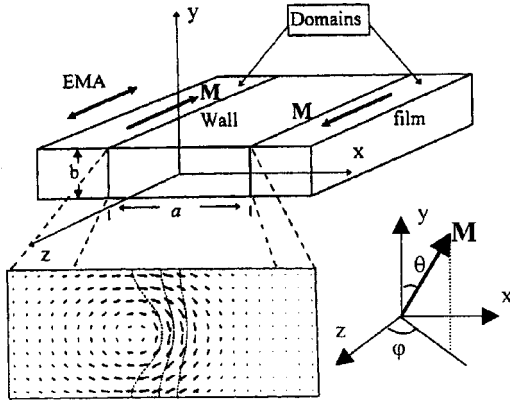


FIG. 1. The geometry of problem and an example of asymmetric vortex structure of a wall obtained for films with basal parameters and $\alpha=0.1$, $b=0.05 \mu\text{m}$. In this and the following figures the arrows denote the projections of \mathbf{v} onto the x - y plane. $M_z < 0$ ($M_z > 0$) to the left (to the right) of the central dashed line. The orientation of \mathbf{M} is described by a polar angle θ and an azimuthal angle ϕ .

models it should be remembered that $\mathbf{M} = \mathbf{M}(x)$ in the region V . The problem of finding $\mathbf{M}(x, y)$ is solved on the basis of a rigorous micromagnetic approach taking into account all the main interactions—the exchange, the dipole-dipole (in continuum approximation), and the magnetoanisotropic interaction. Let us denote the densities of these energies by ε_{ex} , ε_m , and ε_{an} , respectively, where

$$\begin{aligned} \varepsilon_{\text{ex}} &= \frac{A}{M_s^2} \left[\left(\frac{\partial \mathbf{M}}{\partial x} \right)^2 + \left(\frac{\partial \mathbf{M}}{\partial y} \right)^2 \right], \\ \varepsilon_m &= -\frac{1}{2} (\mathbf{M} \cdot \mathbf{H}^{(m)}), \\ \varepsilon_{\text{an}} &= -\frac{K}{M_s^2} (\mathbf{M} \cdot \mathbf{c})^2. \end{aligned} \quad (1)$$

Here A is the exchange interaction parameter, K is the uniaxial magnetic anisotropy constant, M_s is the saturation magnetization, \mathbf{c} is a unit vector along an easy axis, and $\mathbf{H}^{(m)}$ is a magnetostatic field defined as

$$\mathbf{H}^{(m)}(\mathbf{r}) = -\frac{\partial}{\partial \mathbf{r}} \int_V d\mathbf{r}' M_j(\mathbf{r}') \frac{\partial}{\partial x'_j} \frac{1}{|\mathbf{r} - \mathbf{r}'|}. \quad (2)$$

In the framework of the two-dimensional model considered, the energy of a domain wall per unit length along the z axis may be presented in the form

$$\gamma_D = \int_D \int \varepsilon dx dy, \quad (3)$$

where

$$\varepsilon = \varepsilon_{\text{ex}} + \varepsilon_m + \varepsilon_{\text{an}}. \quad (4)$$

To determine $\mathbf{M}(x, y)$ it is necessary to minimize the functional (3) with respect to \mathbf{M} under the condition $\mathbf{M}^2 = \text{const}$ and the following boundary conditions:

$$\left[\mathbf{M}, \frac{\partial \mathbf{M}}{\partial n} \right]_{y=\pm b/2} = 0, \quad (5)$$

$$M_z|_{x=\pm a/2} = \pm M_s, \quad M_x|_{x=\pm a/2} = 0, \quad M_y|_{x=\pm a/2} = 0. \quad (6)$$

In expression (5) $[\dots, \dots]$ stands for a vector product. Minimization of Eq. (3) allows one to find the equilibrium configurations of domain walls and corresponding minimal energy values of γ_0 .

The method of numerical minimization is described in detail in Refs. 1,10. According to it a rectangular grid divides the region D into small cells. The region V is divided into parallelepipeds stretched along the z axis, whose sidewalls are parallel to the coordinate planes $x-z$ and $y-z$. The cells are assumed to have macroscopic, but so small sizes that in every point of each of these parallelepipeds the \mathbf{M} direction may be considered to be uniform. The network approximation of γ_D is discussed in the Appendix.

The numerical calculations were carried out on the grids with various numbers of cells. The maximum mesh of the grid covering the calculation area was 90×30 . The greater number of cells significantly increases the computation time, but only slightly changes the numerical results. The choice of the region D to be computed, i.e., the sizes of a and b , is of a great importance because these sizes essentially depend on the magnetic parameters of a film. The computations were done for $1 \leq a/b \leq 6$. We used the magnitudes $A = 10^{-6} \text{ erg/cm}$, $K = 10^3 \text{ erg/cm}^3$, and $M_s = 800 \text{ emu cm}^{-3}$, which are characteristic of Permalloy films, as the basic parameters of a film. The closeness to unity of the self-consistency coefficient S_0 proposed by Aharoni¹¹ was used as a criterion for the end of the computations.

Figure 1 shows a stable structure of an asymmetric Bloch wall as an example. It was determined for the first time by LaBonte.² First of all, it is seen that the projection of \mathbf{M} varies from domain to domain such that a vortex of magnetization is formed in the x - y plane. The z component of \mathbf{M} also varies. The magnitude of M_z is equal to zero at the central dashed line $y = y_0(x)$ (the center of a wall). Thus, the center of a domain wall corresponds to different x coordinates at different depths of a film. Due to the asymmetry of this line such a wall is called an asymmetric wall. Two other lines at the level $M_z = \text{const}$ (to the left and to the right of the central line) are drawn such that \mathbf{M} rotates about the z axis by about 60° .

In the film shown in Fig. 1 the direction of the \mathbf{M} winding (chirality) is counterclockwise. The walls with this and opposite chirality have the same energy (degeneracy in chirality).

The study of nonlinear dynamics of the domain walls described was done by a direct numerical solution of Landau-Lifshitz equation, written in a dimensionless form

$$(1 + \alpha^2) \frac{\partial \mathbf{u}}{\partial \tau} = -[\mathbf{u}, \mathbf{h}_{\text{eff}}] - \alpha[\mathbf{u}, [\mathbf{u}, \mathbf{h}_{\text{eff}}]], \quad (7)$$

where $\mathbf{u} = \mathbf{M}/M_s$, $\tau = \gamma M_s t$, t is real time, γ is the gyromagnetic ratio, α is a dimensionless Gilbert damping parameter, \mathbf{h}_{eff} is a dimensionless effective field in which the magnetization moves

$$\mathbf{h}_{\text{eff}} = \mathbf{h}_e + \mathbf{h}^{(m)} - h_A (\mathbf{u} \cdot \mathbf{c}) \mathbf{c} + \mathbf{h}, \quad (8)$$

where

$$\begin{aligned} \mathbf{h}_e &= \frac{\partial^2 \mathbf{u}}{\partial \xi^2} + \frac{\partial^2 \mathbf{u}}{\partial \eta^2}, \\ \mathbf{h}^{(m)} &= \mathbf{H}^{(m)}/M_s, \\ \mathbf{h} &= \mathbf{H}/M_s, \\ h_A &= 2K/M_s^2, \\ \xi &= x/b_0, \\ \eta &= y/b_0, \end{aligned} \quad (9)$$

$b_0 = \sqrt{2A}/M_s$, and \mathbf{H} is the external magnetic field. To numerically calculate Eq. (7) with boundary conditions (5) and (6) we use the same spatial grid as was used at the minimization of the functional γ_D . In addition to that, we use the explicit difference scheme (Euler method), added with allowance for the so-called predictor corrector. The distribution \mathbf{u}_0 (i.e., \mathbf{u} in each cell of the spatial grid) is initialized at the moment $\tau=0$. The \mathbf{u}_0 configuration is determined by numerical minimization of the total energy (3) of a wall. At the first stage (predictor) an iteration \mathbf{u}_{n+1} is determined by the formula

$$\mathbf{u}_{n+1}^* = \mathbf{u}_n + \eta \Delta \tau \mathbf{f}(\tau_n, \mathbf{u}_n), \quad (10)$$

where

$$\begin{aligned} \mathbf{f}(\tau_n, \mathbf{u}_n) &= -\frac{1}{1 + \alpha^2} [\mathbf{u}_n, \mathbf{h}_{\text{eff}}(\mathbf{u}_n)] \\ &\quad - \frac{\alpha}{1 + \alpha^2} [\mathbf{u}_n, [\mathbf{u}_n, \mathbf{h}_{\text{eff}}(\mathbf{u}_n)]]. \end{aligned} \quad (11)$$

At the second stage (corrector) the iteration \mathbf{u}_{n+1} is finally determined:

$$\mathbf{u}_{n+1} = \mathbf{u}_n + \Delta \tau \mathbf{f}(\tau_n, \mathbf{u}_{n+1}^*). \quad (12)$$

Here $\Delta \tau$ is the time step. The η parameter can vary within the limits $0 < \eta < 1$. At $\eta=0$ the above-described method degenerates into the explicit Euler difference scheme.¹⁵ In our case the η parameter was chosen, as a rule, to be equal to 0.75. The numerical experiments show that when using the variable adjustable step (see below) in the predictor-corrector method the computation may be accelerated by about seven times in comparison with the Euler method. The results of calculations (e.g., the average over the film thickness veloc-

ity, the magnitude of the period of this velocity at nonstationary motion of a wall, etc.) in both methods coincide with a good accuracy.

The time step $\Delta \tau$ is either chosen constant or variable under the constraint of the maximal rotation angle of the magnetization vector in a cell by a certain small value. In the latter case the step varies by the following algorithm. If the maximal rotation angle of \mathbf{u}_{n+1} with respect to \mathbf{u}_n (over the whole set of the cells) exceeds the given θ_0 value then the step is multiplied by 0.3 (sharply diminishes); otherwise it is multiplied by 1.3 (gradually increases). Our experience has shown that it is quite sufficient to choose $\theta_0=0.01$. The results are insensitive to the further θ_0 reduction. The variable adjustable step allowed us to substantially accelerate the computations and to carry out the calculations for the small values of the damping parameter α .

We anticipated a procedure of introducing random perturbations with arbitrary amplitude at any time instant, and also the possibility of starting from any configuration of the \mathbf{M} . This allows us to evaluate the stability of the solutions obtained. To prevent the reaching of a wall the boundary of the computation region V a shift of the region is anticipated in the course of the wall motion.

Two variants of a shift were studied. In the first, the grid shifts by one cell along the x axis when the ‘‘center of gravity’’ of a wall passes the same distance in this direction. The quantity $\mu^* = u_x^4 + u_y^4$ that characterizes the deviation of the magnetization vector from the quiescent state was chosen as a ‘‘mass.’’ In the second variant, the distribution at each iteration ‘‘shifts’’ backwards such that the ‘‘center of gravity’’ is always in the center of calculation area. This approach allowed us to more accurately determine the critical values of the bifurcation field (the field of transition from the stationary to nonstationary motion of a wall) and to carry out the computations for arbitrary small values of the damping parameter α . This is related to the removal of jumps that appear at a wall shift. It should be emphasized that if the boundary conditions at the calculation area boundaries perpendicular to the x axis are such that the magnetization \mathbf{M} substantially deviates from the z ($-z$) direction in domains so the above definition of the center of gravity may appear to be invalid. Such a situation may either appear, for example, at a presence of nonzero H_x or H_y components of the external field \mathbf{H} or when the 90° domain walls are considered.

III. RESULTS AND DISCUSSION

Let us consider the motion of a domain wall that is induced by the external magnetic field H directed along an easy axis of the magnetization. Previously,⁷⁻⁹ the existence of some critical field H_c (a bifurcation field) was established, below which the motion of a wall proves to be steady state, and the motion with variable velocity occurs above this field. In particular, in some range $H > H_c$ close to H_c the velocity of a domain wall varies periodically. Such a motion corresponds to the periodic rearrangement in the internal structure of a domain wall. As a matter of fact, the subcritical behavior of a domain wall with a vortex internal structure is quite the same as the behavior of the domain wall motion with a one-

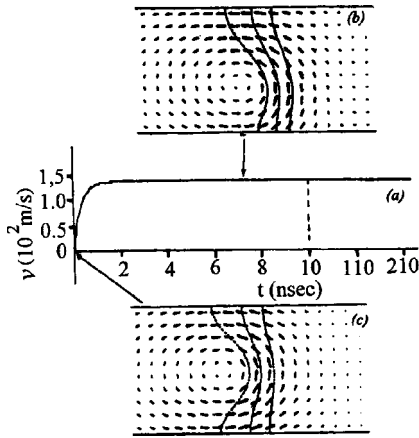


FIG. 2. Instantaneous wall configurations (a),(b) and the dependence of the average (over the film thickness) velocity of a domain wall motion on time at $H=80$ Oe and basal parameters of a film. The portion parallel to abscissa axis corresponds to the stationary wall motion.

dimensional distribution of the magnetization studied in detail in Ref. 12. It is actually related to the violation of a balance of angular momentum, which leads to the precession of the magnetization about an easy axis along with the precession about the direction of a wall motion. The difference is that in the case of a wall with a two-dimensional magnetization distribution the precession of the magnetization about an easy axis is essentially inhomogeneous.^{7,8} In the fields far higher than H_c the wall motion can prove to be much more complicated.⁷ However, such situations will not be considered in this paper.

A. Steady-state motion of a domain wall

The steady-state motion of a domain wall is settled after passing a certain transition process. Hereby two different types of the steady-state motion can be discriminated. Typical examples of transitions to these motions are shown in Figs. 2 and 3 at $\alpha=0.1$. There are shown, in particular, the velocities v of a domain wall motion averaged over the film thickness. In both cases, a vortex shifts to a lower film surface after switching on the external magnetic field. The di-

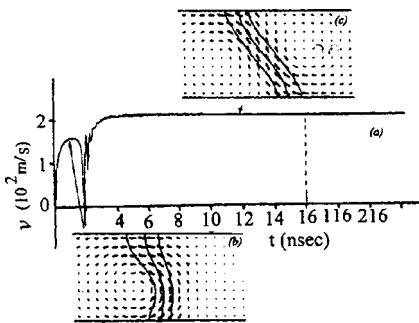


FIG. 3. Instantaneous wall configurations (a),(b) and the dependence of the average (over the film thickness) velocity of a domain wall motion on time at $H=99$ Oe and basal parameters of a film. The portion parallel to abscissa axis corresponds to the stationary wall motion.

rection of the displacement depends on the applied field direction. The situation depicted in Figs. 2 and 3 occurs in the field directed along the z axis and applied to the structure shown in Fig. 1. If the field H sufficiently differs from H_c , then the center of a vortex occupies some equilibrium position between the upper and lower surfaces of a film. By this the transition process terminates, and the domain wall begins to move with a constant velocity. In this case, even a very strong diminishing in α does not lead to any additional features in the domain wall behavior. It is only the range of the fields, in which the considered process occurs, that decreases. If the field H is close to H_c ($H_c - H \ll H_c$), after switching on the field H the vortex at first shifts to the lower surface of a film, and then the asymmetric Bloch wall transforms to the asymmetric Néel wall, depicted in Fig. 3(a). It is just this wall that moves stationary. Its velocity proved to be higher than that of the asymmetric Bloch wall. If now we gradually decrease the damping, then the range of fields in which such a motion occurs also decreases, and quite a novel effect appears as well. In the course of the asymmetric Bloch wall transformation to the asymmetric Néel wall, an excitation of high-frequency oscillations of the wall velocity occurs. A typical example of such a behavior of a wall is shown in Fig. 4.

We fix all the instantaneous configurations of a wall during computation and create an animation on this basis. Looking through this animation gives evidence that the velocity oscillations are related to some parts of a wall that begin to vibrate relative to one another. In particular, with time duration the swing of the central line of the asymmetric Néel wall varies periodically.

As an example, Figs. 4(e) and 4(f) show two configurations of the Néel wall with different swings of the central line. The excitation of the above oscillations occurs due to the appearance of a fast change of nonuniform internal field during the process of the wall rearrangement.

B. Nonstationary motion of a wall

As was noted above, the balance of the angular momentum is violated when $H > H_c$, and the motion of a domain wall ceases to be steady state. Rather complicated transformations in the internal structure of a domain wall develop in the course of its motion. When moving away from the critical field the character of the rearrangement will change. However, it is always possible to select a wide range of magnetic fields, in which the main features of the domain wall dynamic rearrangement will be retained.

As an example, Fig. 5 shows the dependence of the velocity v of a domain wall on time and where the instantaneous domain wall configurations are shown at different stages of transformation. The data was obtained for basic films with $\alpha=0.1$ and in the field $H=100$ Oe. This field is greater than the critical field by about 0.7 Oe. It is seen that if we begin with a configuration of an asymmetric Bloch wall (a), then with time a vortex shifts to the lower surface of the film (b). Then the asymmetric Bloch wall rearranges to the asymmetric Néel wall (c). During this rearrangement the wall velocity decreases, then grows and becomes greater

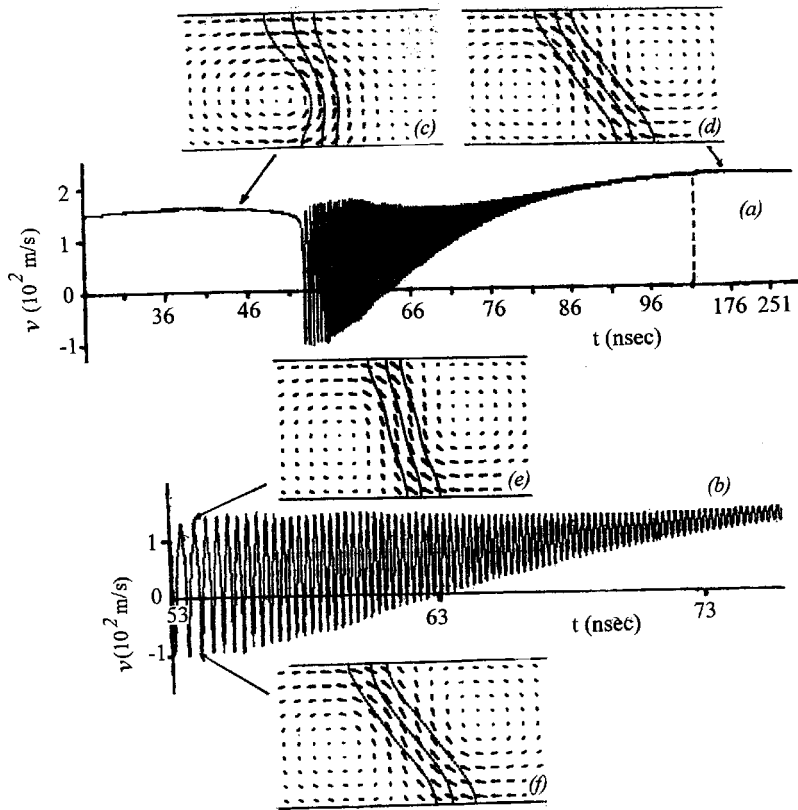


FIG. 4. Instantaneous wall configurations (c),(d) and the dependence of the average (over the film thickness) velocity of a domain wall motion on time at $H=2$ Oe, $\alpha=0.001$, $b=0.05 \mu\text{m}$ and basal parameters of a film. The oscillation velocity part is depicted in more detail in (b).

than the velocity of the asymmetric Bloch wall. After that, the swing of a central line of the asymmetric Néel wall gradually decreases, and the wall structure actually becomes similar to a classical one-dimensional Néel wall (d). At this instant the wall velocity passes through zero and changes sign, then a reverse motion of a wall begins.¹² The structure (d) rearranges to the structure of asymmetric Néel wall (e), but with an opposite slope of a central line, as compared with the structure (c). The swing of this line reaches a maximum. The nature of the domain wall reverse motion is just the same as in one-dimensional walls.¹² It is related to that if the

appearance of the resulting magnetization in the motion direction is necessary for a wall to move. Meanwhile, with the appearance of the \mathbf{M} precession about an easy axis there inevitably appear the states of a wall with a slope of \mathbf{M} relative to the x axis opposite to the initial direction of a domain wall motion.

With further wall moving, the slope angle of the central line again decreases, and near the upper surface of the film a vortex (f) with the chirality opposite to that of the initial vortex (a) is nucleated. A half-period $T/2$ of dynamic rearrangement in the internal structure of a wall terminates when

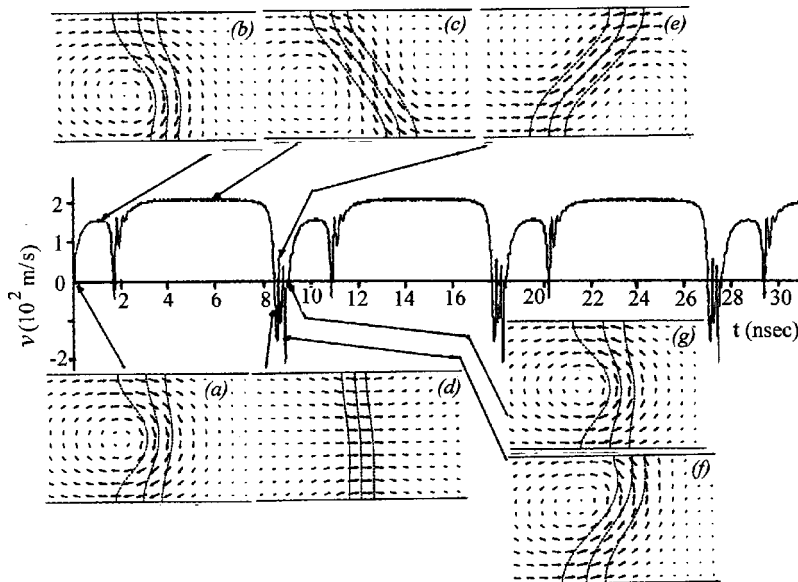


FIG. 5. Instantaneous wall configurations and the dependence of the average (over the film thickness) velocity on time for the film with basal parameters, $b=0.05 \mu\text{m}$, $\alpha=0.1$, and $H=100$ Oe.

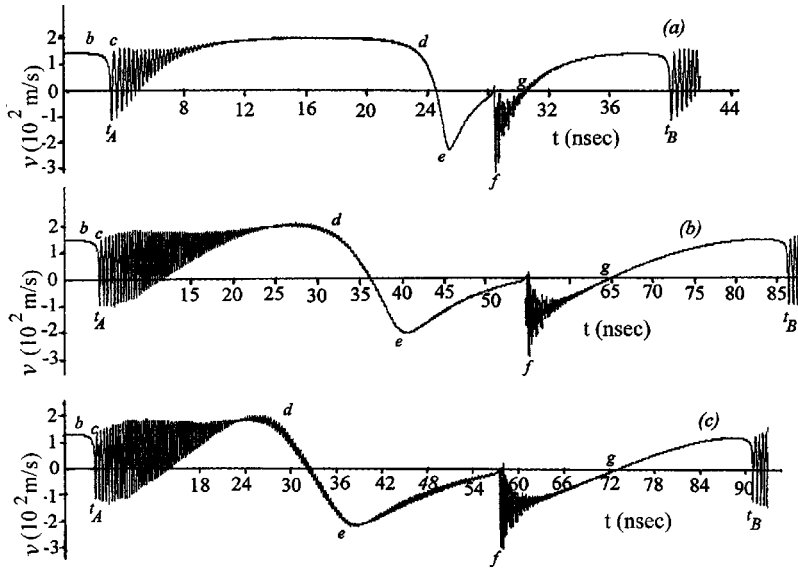


FIG. 6. The dependence of the average (over the film thickness) velocities on time for the film with basal parameters $b=0.05 \mu\text{m}$ and α , H , and H_c : (a) 0.01, 11 Oe, 10.5 Oe; (b) 0.001, 2.6 Oe, 2.5 Oe; (c) 0.0001, 2.2 Oe, 1.9 Oe.

this vortex crosses the film center (g). During the second half-period similar rearrangements of the domain wall structure occur, and at the end of a period the wall chirality returns to the initial one (a). The rearrangements considered correspond to those studied in Ref. 7 at other values of α and H . However, in our case the time dependence of the velocity has quite another form. It has substantially extended the region which corresponds to the existence of asymmetric Néel wall structure. Note that this distinction is related to the choice of H close to the critical field rather than to the choice of α . The extension of this region is caused by the fact that it is rather difficult to overcome the state of a wall with a maximal direction of the magnetization along the x axis [(d) state] in the fields slightly exceeding the critical one. With increasing H above the critical field, the region with a structure of the (c) type gradually narrows, and the time dependence of the velocity becomes similar to that brought out in Ref. 7. Thus, it is clear that the increase in a period of dynamic rearrangement of domain wall internal structure with decreasing external magnetic field down to the critical field is related to the extension of a time interval during which the asymmetric Néel wall exists.

The above-obtained properties do not undergo noticeable changes with passing to the films with lower dampings. However at small dampings, apart from the velocity changes that happen during a whole period T the changes at much shorter time intervals are also seen. We will call them subperiodic velocity oscillations. As an example, Fig. 6 shows the velocity dependence on t for basic film parameters and three different α values.

The subperiodic velocity oscillations are clearly seen in this figure apart from the changes of velocity on a period T ($t_B - t_A = T/2$ in Fig. 6). They are of the same nature as those described when Fig. 4 was discussed. According to this nature, their frequencies do not depend on the field applied along an easy axis, but do depend on the film parameters and its thickness. The specific analysis requires time-consuming computations, and we are going to realize them in the future. The above oscillations are essentially nonlinear. Their fre-

quencies depend on their amplitude. The order-of-magnitude frequency estimation is about 10^{11} Hz.

Leaving aside the subperiodic oscillations the transformations that happen during a period T occur at small α quite similar to the transformations in the case of $\alpha=0.1$. The points (a)–(g) in Fig. 6 correspond to the structures denoted by the same letters in Fig. 5. The velocities correspond to the fields immediately close to the critical fields in each case. Increasing the field to values far exceeding H_c does not substantially change the pattern of a domain wall dynamic behavior. As an example, Fig. 7 shows the velocity dependence for a film with basal parameters and damping $\alpha=0.001$ in the field $H=5$ Oe. This field is about twice the value of H_c . In order to demonstrate the subperiodic velocity oscillations Fig. 8 shows a shorter time interval. This figure also illustrates various oscillation types of the internal structure of a wall by the instantaneous domain wall configurations. Apart from the subperiodic oscillations discussed above it is clearly seen from Fig. 6 that with decreasing damping the fraction of the period T at which a wall moves backward increases. It means that with decreasing damping the average velocity of a wall forward movement gradually decreases, and the wall oscillations related to the nonuniform (over the y axis) precession of the magnetization about the easy axis begin to play the greater and the greater role.

C. Period of dynamic transformations

As is evident from the considerations above, the period T of dynamic transformations in the internal structure of domain walls depends on the external magnetic field. We investigated this dependence for various values of α . Figure 9 shows, as an example, the $T(H)$ dependence for three α values. As it should be on decreasing the external magnetic field and approaching the critical field the period T grows that agrees, in general, with the known one-dimensional model.¹² We compared the field dependence of the period T calculated in this paper in the two-dimensional model of the

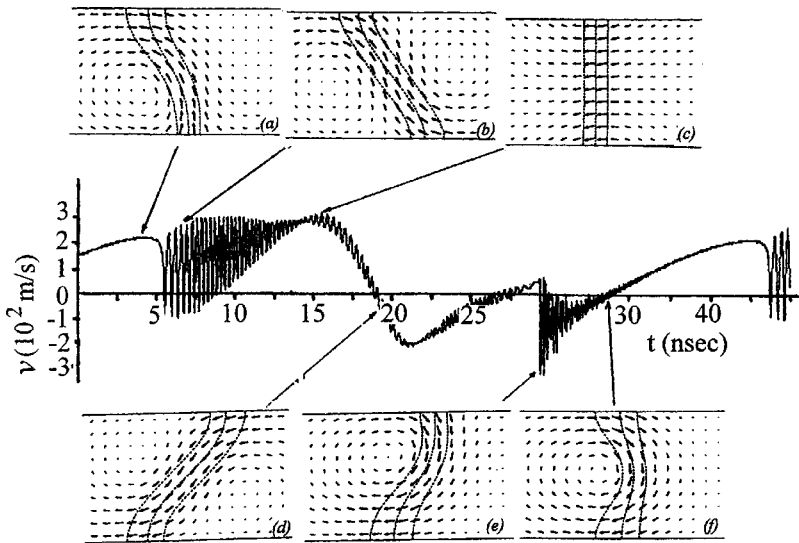


FIG. 7. Instantaneous wall configurations and the dependence of the average (over the film thickness) velocity on time for the film with basal parameters $b=0.05 \mu\text{m}$, $\alpha=0.001$, and $H=5 \text{ Oe}$.

magnetization distribution for basal films with $\alpha=0.1$ and $b=0.05 \mu\text{m}$ with the period $T(H)$ obtained in the one-dimensional model^{12,14}

$$T = \frac{2\pi(1+\alpha^2)}{\omega_c} \frac{1}{\sqrt{\frac{H^2}{H_c^2} - 1}}, \quad (13)$$

where $\omega_c = \gamma H_c$. This comparison is shown in Fig. 10. The solid curve corresponds to Eq. (13), and the points to our numerical experiment. Although giving similar behavior of $T(H)$ the models are seen to qualitatively differ from one another. In other words, the two-dimensional distribution of \mathbf{M} has the character of a singularity of the period T turns out to be different from reciprocal-square root $(H^2/H_c^2 - 1)^{-1/2}$ which is typical for one-dimensional models of a wall. From general considerations an assumption can be inferred that the character of $T(H)$ singularity in the two-dimensional case depends on the thickness and magnetic parameters of the film. However, the elucidation of this interesting question

needs much computation time, and we are going to do it in the future. The above growth of T with decreasing H takes place for arbitrary values of α . It is very important, however, that it is flattening with decreasing α . This circumstance is, in our opinion, favorable for the experimental studies. Note, first of all, that there is no need for great time resolutions in the presence of a long period of dynamic transformations. It seems to be sufficient to carry out the studies near the critical field, since the period T is always great enough in this region. But in the films with $\alpha=0.1$ the critical field is rather high ($H_c \approx 99.3 \text{ Oe}$ for basal films). In the immediate vicinity of this field the period T is undoubtedly large. For example, $T \approx 171.7 \text{ ns}$ at $H=99.33 \text{ Oe}$. If a field is only increased up to 102 Oe , then the period T will fall off to about 11.6 ns . Thus, the field range, in which T is large, is very narrow, and it is difficult to hit such a narrow range. It follows from Figs. 7 and 8, at $\alpha=0.001$ even in the field $H=5 \text{ Oe}$, which is about two times as great as the critical field, the period T still remains great enough, namely, $T \approx 80 \text{ ns}$. As a result, the temporal resolution of the order of 10 ns is required to experimentally reveal a range with periodic variation of the wall velocity. Moreover, there is a great enough reserve for

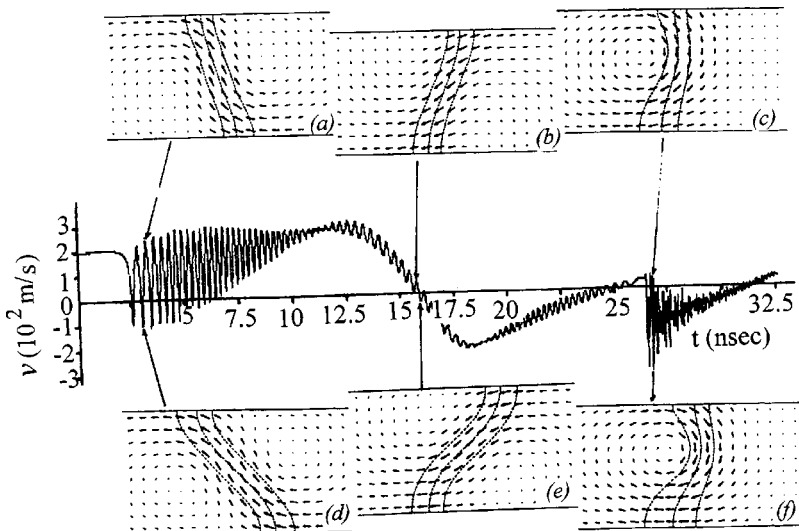


FIG. 8. The dependence of v on T on much less time interval. Instantaneous wall configurations corresponding to minima and maxima of velocity at various stages of a domain wall dynamic rearrangement.

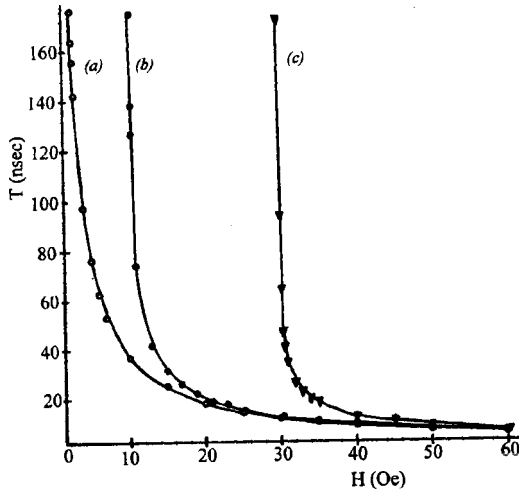


FIG. 9. The dependence of the period of dynamic rearrangements of a domain wall on magnetic field for basal films, $b = 0.05 \mu\text{m}$, and various α : (a) 0.001, (b) 0.01, and (c) 0.03. Circles and triangles are the numerical experiment data, and the curves are the guides for eye.

increasing T by lowering H . The measurements can be carried out, e.g., by the method of high-speed photography in the double- or triple-flash regime for a pulse duration with a flash time of the order of 1 ns to determine the coordinate of instantaneous wall shifting as a function of time $q(t)$. One can obtain the $q(t)$ curve by varying a delay between the first and second flash by about 1 ns, and the third flash may be done at the end of a pulse. At $H < H_c$ no peculiarities will appear on the curve, which should appear in the opposite case $H > H_c$, when the reverse motion is possible to occur. If the time interval t is great enough then several periods can be registered, which allows the determination of $T(H)$ depen-

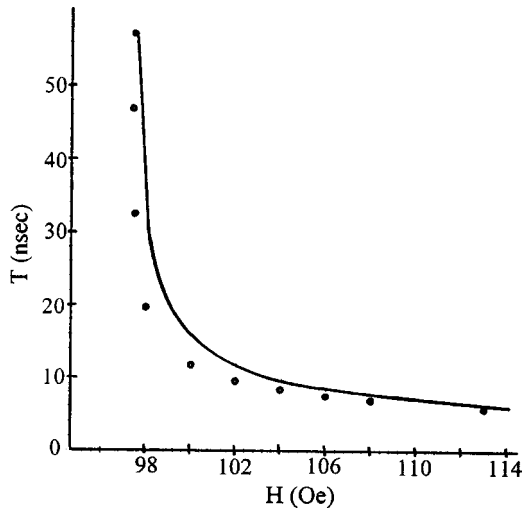


FIG. 10. Comparison of the dependence of the period of dynamic rearrangements of a domain wall calculated by Eq. (13) and numerically computed in the framework of a two-dimensional model. The parameters employed are those for basal films, $\alpha = 0.1$, and $b = 0.05 \mu\text{m}$. Solid curve corresponds to Eq. (13) and circles to the two-dimensional model.

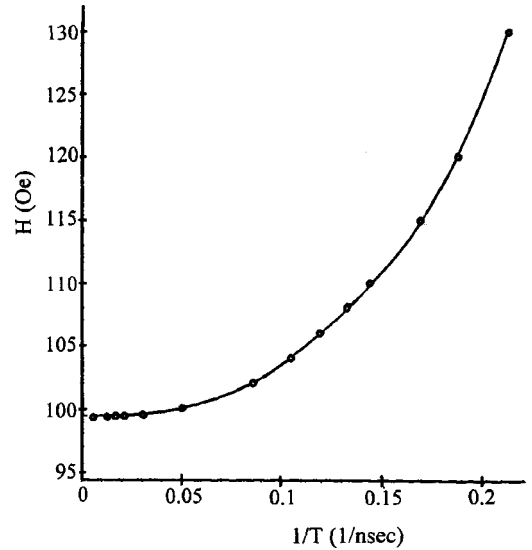


FIG. 11. An example of the H dependence on $1/T$ used for determining the H_c . The parameters employed are those for basal films, $\alpha = 0.1$ and $b = 0.05 \mu\text{m}$.

dence. The snapshots at the beginning and the end of a pulse and the H amplitude variation at $t > T$ will give an opportunity to determine H_c (see below).

It is also very important to choose proper films, the most favorable of which are those with small damping. Note that although we used in our calculations the magnetic parameters close to those of Permalloy films, the above-described behavior retains for the films with other parameters as well. For example, we varied M_s from 400 to 1600 G, K from 10^3 to 10^6 erg/cm³ and obtained a behavior quite similar to that mentioned above.

We also calculated the dependence of a period on the damping α . In accordance with the above data a period grows with increasing α for all $H > H_c$.

D. Critical field of dynamic rearrangement of a domain wall

The most difficult to determine is the critical field H_c . The difficulties are both of the fundamental and computing character; it is a computation-intensive task. Let us explain in short the method for calculating H_c . First of all, for given film parameters the period of dynamic transformations T was calculated as a function of H , then this data was used for constructing the dependence of H on $1/T$. Finally the obtained curve was extrapolated to $1/T = 0$ as shown in Fig. 11 as an example. The ordinate H value was accepted as H_c . This procedure was performed in a wide range of α values and Fig. 12 shows the resulting curve H_c versus α . The behavior of $H_c(\alpha)$ is seen to be almost linear over a wide range of α values, which corresponds to the one-dimensional models data.

However, a substantial distinction from the one-dimensional model, in which $H_c/\alpha = 2\pi M_s$ ($\sim 5 \times 10^3$ emu cm⁻³ for considered basal films with the thickness $0.05 \mu\text{m}$) is that the two-dimensional model gives much smaller values of $H_c/\alpha \sim 10^3$ emu cm⁻³ for similar films. Moreover, our previous numerical calculations⁹ show

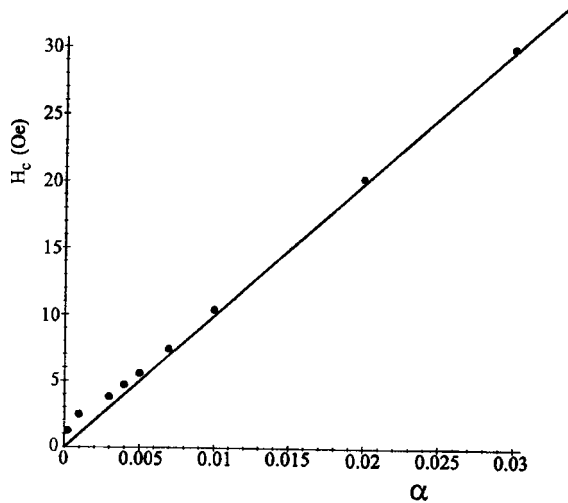


FIG. 12. The dependence of the critical field H_c on α for the films with basal parameters and $b=0.05 \mu\text{m}$. Circles are the numerical experiment data, and a straight line corresponds to the linear dependence $H_c = P\alpha$ with $P=10^3 \text{ Oe}$.

that H_c/α depends on the film thickness. These features can be easily understood by remembering¹² that the very existence of a critical field is related to the finiteness of angular momentum caused by the $H_x^{(m)}$ component of magnetostatic field.

In a film, in contrast to an infinite crystal considered by Schryer and Walker,¹² the wall dimensions are finite along the direction perpendicular to the film surface. This induces the $H_x^{(m)}$ component of the field, caused by the magnetostatic poles that inevitably appear with appearance of the magnetization precession at the wall surfaces perpendicular to the motion direction and it will be different in each film. The specific character of the \mathbf{M} distribution is surely important. This field in a film will depend on its thickness, which will lead to the thickness dependence of H_c . In such a case, the magnitude H_c/α would seem to grow approaching the value $2\pi M_s$, but, as our calculations show, the value of H_c/α in more thick films may become even less than the value mentioned above ($\sim 10^3 \text{ emu cm}^{-3}$). The latter is related to the fact that in thick films the scenario of the dynamic rearrangement of the internal structure of a domain wall becomes complicated as a greater number of vortices are involved in the rearrangement than before. This is in agreement with the results of Ref. 7. The appearance of several vortices with different chirality leads to the splitting up of the magnetostatic poles at the surface of a film perpendicular to the motion direction, which naturally diminishes $H_x^{(m)}$ and, as a consequence, H_c .

We relate the nonlinear deviations from the linear $H_c(\alpha)$ dependence that appear at small α to the development of subperiodic oscillations which effect the average (over time) values of $H_x^{(m)}$. It should be noted that the study of very small damping, such as less than 10^{-4} , needs very great computation time, and it is difficult to say whether the observed deviations play any role in the $H_c \rightarrow 0$ transition at $\alpha \rightarrow 0$.

In spite of the fact that a critical field is the most difficult magnitude to compute we believe that its experimental study as a function of various film parameters will prove to be rather simple. Indeed, the wall velocity grows with growing H up to the critical field. Above $H=H_c$, the dynamic rearrangement in the internal structure of a wall develops, and reverses its motion. Due to conventional experimental methods¹³ the velocity is measured at the time intervals far exceeding a period T of the wall dynamic rearrangement so that it is the average velocity (over the period T) that is measured in the field H . Since with increasing field, as our studies show, the period decreases and the relative contribution of reverse motions increases, so the measured velocity should fall off with increasing field. Thus, a maximum of the velocity measured has to be observed at $H=H_c$. This maximum was really observed in experiment.¹³ Hence, by measuring the velocity maximum in the field dependence at various parameters of a film one can determine the critical field as a function of these parameters.

IV. CONCLUSIONS

We investigated the nonlinear and, in general, nonstationary dynamics of domain walls in magnetic films with an in-plane anisotropy and rather small damping α (down to 10^{-4}). Such studies succeeded only due to the introduction of variable time step.

Two different types of the stationary wall motion are revealed. The first is related to the equilibrium state of a wall vortex at a certain distance from the film center. The second type, that appears in the fields H close to the critical one, is related to the appearance of the dynamically stable asymmetric Néel wall. Since the velocity of asymmetric Néel wall is usually higher than that of the asymmetric Bloch wall, the dependence of v on H will be nonlinear in the range $H \lesssim H_c$ and different from that predicted for the materials with a quality factor $Q < 1$ in the framework of one-dimensional model of a wall.¹²

In the fields above the critical one, the nonstationary behavior of a domain wall was established to be more complicated at small damping ($0.0001 < \alpha < 0.02$) than for large α values (e.g., at $\alpha=0.1$). For small damping, along with a periodic dynamic rearrangement of the internal structure of domain walls occurring during large periods T (up to several dozens of nanoseconds) there also appear high-frequency (subperiodic) oscillations of velocity of domain wall motion (with a period $\approx 10^{-2} \text{ ns}$) at certain portions of the period T .

These oscillations are established to be related to various types of vibrations of some parts of domain walls relative to one another. They appear every time when a fast change of the strength of inhomogeneous internal magnetic field occurs due to the rearrangement in the wall internal structure. At different portions of the period T the form of oscillations proves to be different but they are nonlinear in every case, and their period varies with varying amplitude. The external magnetic field H applied along an easy axis and forcing a domain wall to move does not effect their frequency. The increase in H leads to the high-frequency oscillations of the internal structure of a wall begin to exhibit themselves on the

greater and the greater parts of a period T of the main rearrangement of a domain wall.

Also we investigated the dependence of the period T of the basic rearrangement of a domain wall on the strength of external magnetic field for various values of the damping α . In fields $H > H_c$ at any value of α the period grows with decreasing H such that a conclusion on the singular character of $T(H)$ may be inferred by analogy with the one-dimensional model of a wall. In this connection, it seems straightforward to observe the velocity variation due to the periodic dynamic rearrangements in the fields close to the critical one. If the damping is not so small ($\alpha \sim 0.1-0.02$), however, the increase in the external magnetic field even by several percent may decrease the period T by an order of magnitude which makes the time resolution difficult. It would be much more favorable to observe the velocity oscillations at small damping ($\alpha < 0.005$). In this case, even with increasing of the external field up to values exceeding the critical field it is quite possible to deal with periods of dynamic rearrangement equal to hundreds of nanoseconds. Another advantageous aspect for experimental investigations of dynamic rearrangement of domain walls in films with small damping is the smallness of external magnetic field (of an order of several Oe) at which this rearrangement occurs.

Finally, we studied for the first time the critical fields and showed that, although the α dependence of H_c in a wide range of α is close to the linear one, the very magnitude of H_c/α appears to be much smaller than follows from the results of one-dimensional model. The studies carried out show that with decreasing α not only the field range, in which a wall moves stationary, narrows, but simultaneously the backward motions of a wall begin to play a greater role. In the $H > H_c$ field range the velocity of a wall's forward motion gradually decreases, and the wall oscillations related to the nonuniform magnetization precession about an easy axis and as well as the subperiodic vibrations of some parts of a wall begin to play a greater role in the motion of the wall.

ACKNOWLEDGMENTS

We are grateful to Dr. V. V. Volkov (Ioffe Physicotechnical Institute, Russian Academy of Sciences, Politekh-nicheskaya ul. 26, St. Petersburg, 194021 Russia) for useful remarks and discussion. This work was supported by the Russian Foundation for Basic Research, Project No. 99-02-16279.

APPENDIX A: NUMERICAL SOLUTION OF THE STATIC PROBLEM

We used the network approximation for finding the static magnetization distribution. The whole region V was subdivided into $L \times P$ rectangular prisms expanded along the z axis. Denote the sizes of an (l, p) cell along x and y axes by Δx_l and Δy_p , respectively, and use in what follows the dimensionless quantities $\Delta \xi_l = \Delta x_l/b$ and $\Delta \eta_p = \Delta y_p/b$. The

magnetization distribution will be described by the dimensionless unit vector $\mathbf{u} = \mathbf{M}/M_s$. The directional cosines of the magnetization vector \mathbf{u} belonging to the (l, p) cell are denoted by α_{lp} , β_{lp} , and γ_{lp} respectively, and consider the vector $\mathbf{u} = (\alpha_{lp}, \beta_{lp}, \gamma_{lp})$ to be constant within each cell. In the network approximation, the contributions to γ_D from the exchange ϵ_{ex} and magnetoanisotropic ϵ_{an} interactions, where

$$\epsilon_{\text{ex}} = \int_D \int \epsilon_{\text{ex}} dx dy, \quad (\text{A1})$$

$$\epsilon_{\text{an}} = \int_D \int \epsilon_{\text{an}} dx dy, \quad (\text{A2})$$

may be presented in the following form:

$$\epsilon_{\text{ex}} = \sum_{p=0}^{P-1} \Delta \eta_p \left\{ \sum_{l=1}^{L-1} \frac{1 - N_{l-1,p;l,p}}{\Delta \xi_l} + \frac{1 + \gamma_{0p}}{\Delta \xi_0} + \frac{1 - \gamma_{l-1,p}}{\Delta \xi_l} \right\} + \sum_{l=0}^{L-1} \Delta \xi_l \sum_{p=0}^{P-1} \frac{1 - N_{l,p-1;l,p}}{\Delta \eta_p}, \quad (\text{A3})$$

$$\epsilon_{\text{an}} = \frac{Kb^2}{2A} \sum_{p=0}^{P-1} \Delta \eta_p \sum_{l=0}^{L-1} \Delta \xi_l (1 - \gamma_{lp}^2). \quad (\text{A4})$$

When writing Eq. (A3) we represented the derivatives with respect to coordinates by finite differences and also used the relation $\mathbf{M}^2 = M_s^2$. As for the contribution to γ_D from the magnetostatic energy

$$\epsilon_m = \int_D \int \epsilon_m dx dy, \quad (\text{A5})$$

it may be represented as

$$\epsilon_m = -\frac{b^2 M^2}{4A} \sum_{l=0}^{L-1} \sum_{p=0}^{P-1} \sum_{i=0}^{L-1} \sum_{j=0}^{P-1} [A_{lpij} \alpha_{lp} \alpha_{ij} + B_{lpij} \alpha_{lp} \beta_{ij} + B_{lpij} \beta_{lp} \alpha_{ij} + C_{lpij} \beta_{lp} \beta_{ij}], \quad (\text{A6})$$

where

$$A_{lpij} = S(A^f), \quad (\text{A7})$$

$$B_{lpij} = S(B^f), \quad (\text{A8})$$

$$C_{lpij} = -A_{lpij} + 4\pi(a_{l+1} - a_l)(b_{l+1} - b_l) \delta_{li} \delta_{pj}, \quad (\text{A9})$$

$$S(D^f) = R[D^f(a_{l+1}, b_{p+1})] - R[D^f(a_l, b_{p+1})] - R[D^f(a_{l+1}, b_p)] + R[D^f(a_l, b_p)], \quad (\text{A10})$$

$$R[D^f(x, y)] = R^f(x, y, a_{i+1}, b_{j+1}) - R^f(x, y, a_i, b_{j+1}) - R^f(x, y, a_{i+1}, b_j) + R^f(x, y, a_i, b_j). \quad (\text{A11})$$

In Eqs. (A10) and (A11) D should be replaced by A and B . Here S and R are the formal operations, whose application to the functions A^f and B^f leads to the numbers A_{lpij} and B_{lpij} calculated as a sum of sixteen terms of the type

$$A^f(x, y, a, b) = 2(x-a)(y-b) \arctan \frac{y-b}{x-a} + 1/2[(x-a)^2 + (y-b)^2] \ln[(x-a)^2 + (y-b)^2] \quad (\text{A12})$$

and

$$B^f(x, y, a, b) = [(x-a)^2 + (y-b)^2] \arctan \frac{y-b}{x-a} - (x-a) \times (y-b) \ln[(x-a)^2 + (y-b)^2], \quad (\text{A13})$$

where x and y should be replaced by the boundaries of the lp cell, and a and b by the boundaries of the ij cell.

¹A. Hubert, *Theorie der Domänenwänden in Geordneten Medien* (Springer-Verlag, New York, 1974).

²A. E. LaBonte, *J. Appl. Phys.* **40**, 2450 (1969).

³A. Hubert, *Phys. Status Solidi B* **32**, 519 (1969).

⁴D. Hohersall, *Phys. Status Solidi B* **51**, 529 (1972).

⁵S. Tsukahara and H. Kavakatsu, *J. Phys. Soc. Jpn.* **32**, 1993 (1972).

⁶M. R. Scheinfein, *Phys. Rev. B* **43**, 3395 (1991).

⁷S. V. Yuan and H. N. Bertram, *Phys. Rev. B* **44**, 12 395 (1991).

⁸B. N. Filippov and L. G. Korzunin, *Fiz. Tverd. Tela (St. Petersburg)* **38**, 2442 (1996).

⁹B. N. Filippov and L. G. Korzunin, *Phys. Met. Metallogr.* **83**, 584 (1997).

¹⁰B. N. Filippov and L. G. Korzunin, *Phys. Met. Metallogr.* **75**, 359 (1993).

¹¹A. Aharoni, *J. Appl. Phys.* **39**, 861 (1968).

¹²N. L. Schryer and L. R. Walker, *J. Appl. Phys.* **45**, 5406 (1974).

¹³D. S. Bartran and H. C. Bourne, Jr., *IEEE Trans. Magn.* **MAG-8**, 743 (1972).

¹⁴B. N. Filippov and A. P. Tankeev, *Dynamical Effects in Ferromagnets with Domain Structure* (Nauka, Moscow, 1987).

¹⁵G. I. Marchuk, *Methods of Calculus Mathematics* (Nauka, Moscow, 1989).